

# Connexin46fs380 Causes Progressive Cataracts

Viviana M. Berthoud, Peter J. Minogue, Helena Yu, Joseph I. Snabb, and Eric C. Beyer

Department of Pediatrics, University of Chicago, Chicago, Illinois, United States

Correspondence: Viviana M. Berthoud, Department of Pediatrics, University of Chicago, 900 East 57th Street, KCBD-5, Chicago, IL 60637, USA; vberthou@peds.bsd.uchicago.edu.

Submitted: June 12, 2014

Accepted: July 28, 2014

Citation: Berthoud VM, Minogue PJ, Yu H, Snabb JI, Beyer EC. Connexin46fs380 causes progressive cataracts. *Invest Ophthalmol Vis Sci*. 2014;55:6639–6648. DOI:10.1167/iov.14-15012

**PURPOSE.** Although many connexin46 (Cx46) mutants have been linked to inherited human cataracts, there are no adequate animal models for their study. The current experiments were designed to characterize the consequences of expression of one such mutant, Cx46fs380, in the mouse lens.

**METHODS.** Mice expressing Cx46fs380 were generated by a knockin strategy. Levels and distribution of specific proteins were analyzed by immunoblotting and immunofluorescence.

**RESULTS.** Dark-field microscopy revealed that lenses of young heterozygous and homozygous Cx46fs380 mice did not have opacities, but they developed anterior nuclear cataracts that became more severe with age. Immunofluorescence and immunoblotting showed that Cx46 was severely reduced in both heterozygous and homozygous Cx46fs380 lenses at 1 month of age, whereas immunoreactive connexin50 (Cx50) was moderately decreased. The reduction in Cx50 became more severe in older lenses. The solubilities of crystallins from young wild-type and fs380 mice were similar, but older fs380 lenses exhibited abnormalities of abundance, solubility, and modification of some crystallins.

**CONCLUSIONS.** Major decreases in connexin levels precede the development of cataracts. These mice represent a useful model for elucidation of the progression of lens abnormalities during cataractogenesis especially as caused by a mutant connexin.

Keywords: cataract, connexin, gap junction, crystallins

Cataracts are a leading cause of visual impairment.<sup>1–3</sup> The pathogenesis of cataracts of different etiologies may be elucidated by studying the forms caused by single gene mutations. Congenital cataracts have been linked to mutations of genes encoding many of the major lens proteins, including crystallins, membrane proteins, and transcription factors.<sup>4,5</sup> Most bilateral nonsyndromic congenital cataracts are inherited according to an autosomal dominant pattern.<sup>5</sup>

The lens fiber connexins, Cx46 (*GJA3*) and Cx50 (*GJA8*), are prominent among the genes whose mutations cause cataracts.<sup>6</sup> Connexins form intercellular channels clustered within structures called gap junctions that allow the direct transfer of cytoplasmic ions and small (<1 kDa) solutes between adjacent cells. Because adult lens cells have no direct blood supply, gap junction channels are critical for the circulation of water and solutes within the lens.<sup>7,8</sup> Their important contributions to lens homeostasis and transparency are corroborated by the development of cataracts in mice with homozygous deletion of either lens fiber connexin.<sup>9,10</sup>

Unfortunately, detailed studies of the pathways involved in the pathogenesis of human mutation-linked cataracts or the time course of their development are not feasible using human lenses, because cataracts are not removed until they are rather severe, and the integrity of the lens is typically destroyed during extraction. Therefore, it is necessary to develop and utilize model systems for their study.

We and other investigators have used exogenous expression systems to characterize the behavior of human lens connexin mutants associated with autosomal dominant cataracts. These studies have shown that most of the mutants do not traffic properly to the plasma membrane and/or do not form functional channels.<sup>6</sup> One such mutant (Cx46fs380) has a

frame shift (caused by a nucleotide insertion) within the coding region of Cx46 leading to the production of an 87 amino acid long aberrant sequence in the carboxyl terminus starting from amino acid residue 380.<sup>11</sup> This abnormal sequence (which contains a retention/retrieval signal) causes the localization of fs380 within the cytoplasmic biosynthetic/secretory pathway.<sup>12</sup>

Several mouse models have been developed to replicate human connexin mutations that cause diseases of some other organ systems.<sup>13–17</sup> However, there are few mouse lines that mimic the human lens Cx50 mutants<sup>18,19</sup> and none that correspond to human Cx46 mutations. Therefore, to examine the effects of Cx46fs380 within the intact organism, we generated a mouse model in which we replaced the DNA sequence encoding wild-type Cx46 with a DNA sequence encoding Cx46fs380.

In this paper, we describe the results of our studies of the gross appearance of the lenses of these mice and several of their cellular and biochemical characteristics.

## MATERIALS AND METHODS

### Generation of Cx46fs380 Knockin Mice

Cx46fs380 mice were generated as detailed in the Supplementary Methods such that the region encoding the first 365 amino acids of mouse Cx46 was followed in-frame by the DNA sequence coding for the aberrant amino acid sequence in human Cx46fs380.<sup>11</sup> These mice were maintained in a mixed 129/C57BL6 background that was free of phakinin (CP49) mutations. Correct genomic DNA recombination was confirmed by Southern blotting, and mutant expression was confirmed by RT-PCR. All animal procedures were performed

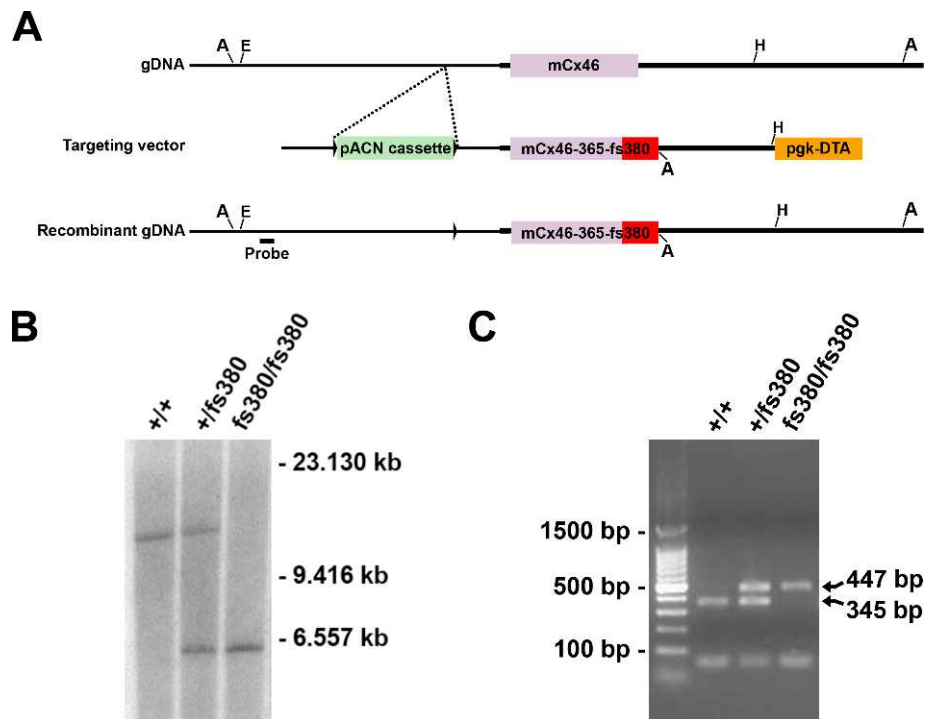


**FIGURE 1.** Generation of knockin Cx46fs380 mice. (A) Diagram showing a portion of chromosome 14 (gDNA) containing the coding region of mouse Cx46 and adjacent segments, the targeting vector, and the expected recombinant genomic DNA. The targeting vector contained the self-excising pACN cassette flanked by loxP sites (right-pointing triangles) and the A subunit of the diphtheria toxin gene under the control of the phosphoglycerate kinase 1 promoter (pgk-DTA) for negative selection. The locations of *AvrII* (A), *EcoRI* (E), and *HindIII* (H) restriction sites are indicated. (B) Southern blot of genomic DNA prepared from tail biopsies of wild-type (+/+), Cx46fs380 heterozygous (+/fs380), and homozygous (fs380/fs380) mice digested with *AvrII* using a 5' UTR probe (short bar in [A]). The expected wild-type *AvrII* fragment is 11,032 bp, and the expected recombinant *AvrII* fragment (after pACN cassette excision) is 5921 bp. (C) Gel containing electrophoresed products from RT-PCR performed using primers flanking the introduced aberrant fs380 DNA sequence and total lens RNA from wild-type (+/+), heterozygous (+/fs380), and homozygous (fs380/fs380) mice showing the presence of the wild-type amplicon (345 bp) in the samples from wild-type and heterozygous animals and of the fs380 amplicon (447 bp) in RNA from heterozygous and homozygous mice. The first lane shows the DNA bands of a 100-bp ladder. The migration positions of the 1500, 500, and 100 bp standards are indicated on the left.

in accordance with the ARVO Statement for the Use of Animals in Ophthalmic and Vision Research and followed the Institutional Animal Care and Use Committee guidelines from the University of Chicago.

### Light Microscopy Analysis

Dark-field photomicrographs of lenses from different-aged mice were obtained using a Zeiss Stemi-2000C dissecting scope (Carl Zeiss, München, Germany).

### Immunoblotting and Immunofluorescence

Connexins, other lens membrane proteins, and crystallins were detected by immunoblotting<sup>19–21</sup> and immunofluorescence<sup>19,22</sup> as previously described. (See the Supplementary Methods for a detailed description.)

## RESULTS

### Generation of Cx46fs380 Knockin Mice

To study the effects of expression of the Cx46 mutant, Cx46fs380 (called fs380 for simplicity), we used homologous recombination to generate “knockin” mice expressing the mutant protein from the Cx46 locus (Fig. 1A). Southern blot hybridization demonstrated successful homologous recombination. A single band of 11,032 bp was detected in samples from wild-type animals. Samples from homozygous fs380 mice showed a 5921-bp hybridizing band (expected for fs380

recombination), whereas samples from heterozygous animals showed two hybridizing bands with sizes corresponding to the wild-type and fs380 alleles (Fig. 1B).

Expression of wild-type and mutant Cx46 messenger RNAs was confirmed by RT-PCR. We obtained an amplicon of the expected wild-type size (345 bp) in samples from wild-type mice and a DNA band of the expected fs380 size (447 bp) in samples from homozygous fs380 mice. Amplicons of both sizes were detected in heterozygous animals (Fig. 1C). The correct identities of these amplicons were confirmed by sequencing.

### Cataracts Develop Late in fs380-Expressing Mice

To determine whether fs380 expression led to cataract formation, we examined lenses from heterozygous and homozygous fs380 animals under dark-field illumination and compared them to those of wild-type mice. Lenses of heterozygous and homozygous fs380 mice showed no obvious opacities at 1 month of age (not shown). Cataracts were detected in homozygous fs380 animals at 2 months of age and thereafter. Cataracts were first observed in some heterozygotes at 4 months of age and were found in all heterozygous mice at older ages (Fig. 2). The cataract was anterior nuclear and was initially composed of small opacities that followed a “Y” shape. It became more complex and progressively worse with age (Fig. 2). Lenses from homozygous mice and many older heterozygotes also showed concentric rings that were particularly evident at 7.7 months (Fig. 2). There was no apparent

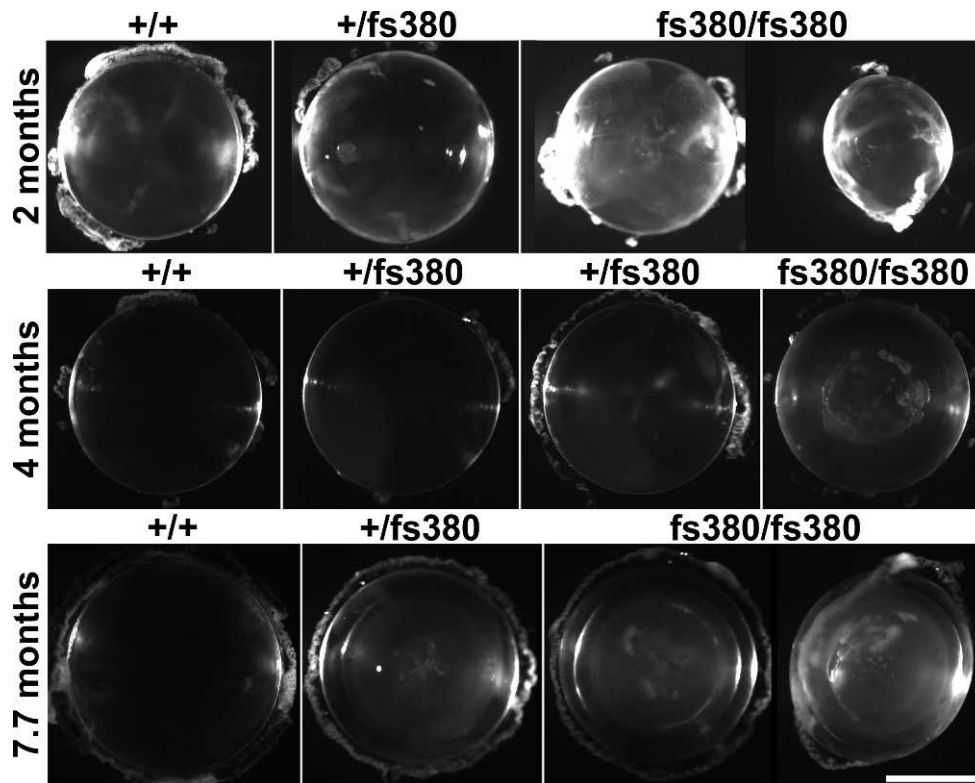


**FIGURE 2.** Expression of Cx46fs380 leads to progressive formation of cataracts. The lenses from wild-type (+/+) and Cx46fs380 heterozygous (+/fs380) and homozygous (fs380/fs380) mice at 2, 4, and 7.7 months of age were photographed using dark-field illumination. For age 4 months, lenses from two different heterozygous mice are shown to illustrate that some (*left*: +/fs380) had no opacities, while others (*right*: +/fs380) had small cataracts. For 2 and 7.7 months, homozygous lenses are shown from different views to illustrate the anterior nuclear position of the cataracts. When photographing the 2-month-old homozygous lenses, the illumination was adjusted to better demonstrate the cataract. Scale bar: 1.18 mm, except for the side view of the 2-month-old fs380/fs380 lens in which it is 1.48 mm.

difference in lens size between wild-type animals and mice expressing fs380 (Fig. 2).

### Expression of fs380 Decreases Lens Fiber Connexins

To test whether expression of fs380 affected Cx46 levels, we performed immunoblots on total lens homogenates prepared from 1-month-old mice. Levels of Cx46 were dramatically decreased in both heterozygous and homozygous fs380 mice (Fig. 3). They comprised <2% and <1% of wild-type values in heterozygotes and homozygotes, respectively (Fig. 3).

The dramatic decrease in Cx46 was also evident in lens sections studied by immunofluorescence staining using anti-Cx46 antibodies (and TRITC-conjugated phalloidin [Sigma-Aldrich Corp., St. Louis, MO, USA] to delineate the cell margins). Sections from wild-type lenses showed intense Cx46-immunoreactive puncta in many fiber cell layers that extended from the periphery toward the center of the lens. In contrast, only a few Cx46-immunoreactive puncta of lower intensity were detected in heterozygous fs380 lenses, and nearly none were observed in homozygotes (Fig. 4).

We also examined the immunolocalization of Cx46 in the lens epithelium, because its distribution in lens epithelial cells has not previously been reported (although in Cx46 knockout [Cx46KO or Cx46-null] mice, in which the  $\beta$ -galactosidase sequence disrupts much of the Cx46 coding region, low levels of Cx46 expression have been detected by using  $\beta$ -galactosidase staining of lens sections).<sup>9</sup> We detected some Cx46 immunoreactivity in epithelial whole mounts of wild-type

lenses. Some of the Cx46-immunoreactive puncta were interspersed with N-cadherin immunoreactivity confirming its plasma membrane localization; however, many of the bright immunoreactive puncta did not colocalize with N-cadherin (Fig. 5A; shown at higher magnification in Supplementary Figs. S1A–C). Since lens epithelial cells express Cx43,<sup>23</sup> we performed double-label immunofluorescence and demonstrated that only a few of the Cx46 puncta overlapped with Cx43 (Fig. 5B, Supplementary Figs. S1D–F).

The presence of Cx46 in the epithelium of wild-type lenses led us to test whether expression of fs380 also affected epithelial Cx46. Double-label immunofluorescence showed the near total absence of Cx46 immunoreactivity in whole mounts of lens epithelia from heterozygous and homozygous fs380 mice without obvious changes in the distribution of Cx43 (Fig. 5). Because expression levels of Cx46 in these cells were low and most of the Cx46 puncta localized intracellularly, it is possible that Cx46 resides in a compartment that is not accessible for oligomerization with Cx43 as occurs in osteoblastic cells,<sup>24</sup> and therefore expression of Cx46fs380 had little effect (if any) on Cx43.

Because Cx50 is coexpressed with Cx46 in lens fiber cells and these two connexins can co-oligomerize,<sup>25,26</sup> we tested whether expression of fs380 affected Cx50. Immunoblots of lens homogenates showed decreased levels of Cx50 in heterozygous and homozygous fs380 lenses compared with the values obtained from wild-type lenses. At 1 month of age, lenses of heterozygous and homozygous mice contained on average 63% and 29% (respectively) of the amounts in wild-type lenses (Fig. 6). This decrease became more pronounced

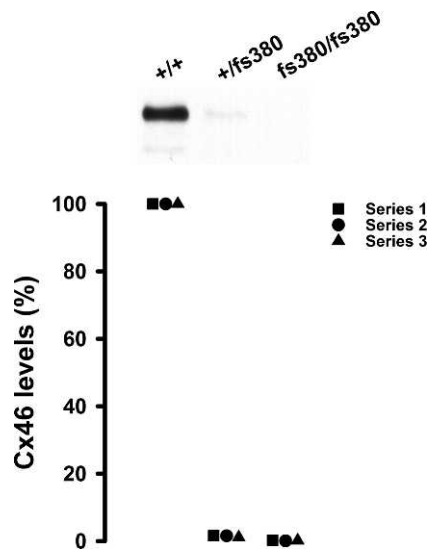


**FIGURE 3.** Levels of immunoreactive Cx46 are dramatically decreased in Cx46fs380-expressing lenses. Immunoblot shows the levels of immunoreactive Cx46 in total lens homogenates from 1-month-old wild-type (+/+) and Cx46fs380 heterozygous (+/fs380) and homozygous (fs380/fs380) mice. The *graph* shows the densitometric values of the bands obtained in three independent experiments expressed as percentages of the values obtained in wild-type animals. The data in each independent experiment (■, Series 1; ●, Series 2; ▲, Series 3) have been offset horizontally to show the values of heterozygotes and homozygotes in all experiments.

with age. At 7.7 months of age, Cx50 levels were reduced on average to only 29% (heterozygotes) and 3% (homozygotes) of wild-type values (Fig. 6).

We analyzed whether the distribution of lens Cx50 was affected by expression of fs380 by performing double-labeling immunofluorescence. In heterozygous and homozygous fs380 animals, Cx50 localized to puncta at appositional membranes in a distribution similar to that seen in wild-type (Fig. 7, Supplementary Fig. S2). However, the intensity of the Cx50-immunoreactive signal was decreased in sections from 1-month-old heterozygous and homozygous fs380 mice (Fig. 7). This diminution was particularly evident in the most superficial cortical fiber cells (Fig. 7, left). In wild-type lenses, these cells contained many bright Cx50 puncta that appeared close together; in contrast, mutant lenses (especially those of homozygotes) contained fewer bright puncta, and the puncta appeared farther apart from each other (Fig. 7). In lenses of 5.6-month-old mice, the Cx50-immunoreactive puncta were smaller, dimmer, and more sparsely distributed in both heterozygous and homozygous fs380 lenses as compared with wild-type lenses (Supplementary Fig. S2).

### Expression of Cx46fs380 Affected Some Other Plasma Membrane Proteins

We also evaluated the possible effect of fs380 expression on levels and distribution of the major intrinsic protein, aquaporin0 (AQP0). Although exhibiting some variability among different individuals of the same genotype, average levels of AQP0 were not very different between wild-type and heterozygous or homozygous fs380 mice (Fig. 8A). The distributions of AQP0 were similar in fs380 and wild-type lenses (Fig. 8B).

Additionally, we determined levels of the cell adhesion molecule, N-cadherin, which is present in all lens cells.<sup>27</sup> No

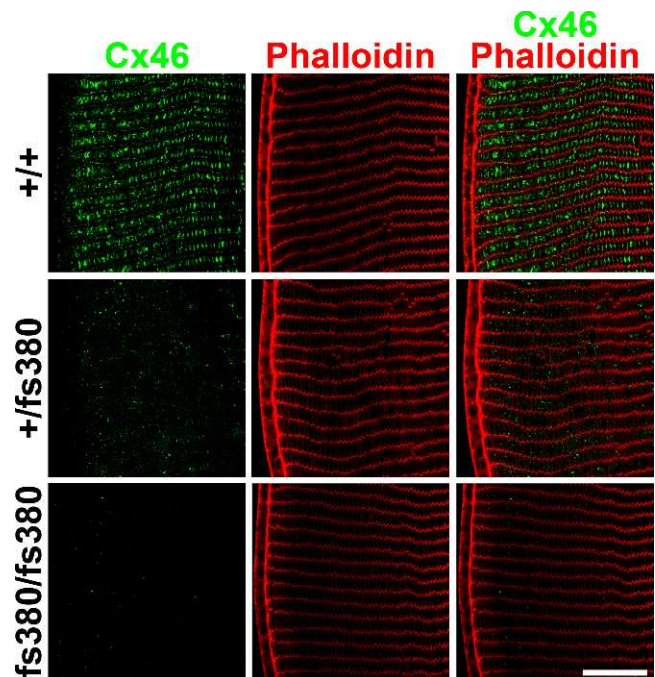


**FIGURE 4.** Immunoreactive Cx46 is severely decreased in fiber cells of Cx46fs380-expressing lenses. Confocal images show the distributions of immunoreactive Cx46 (*green*) and filamentous actin (phalloidin, *red*) in cross sections from lenses of wild-type (+/+), heterozygous (+/fs380), and homozygous (fs380/fs380) mice at 1 month of age. The merged images for the two fluorescence signals are shown on the right. Scale bar: 39  $\mu$ m.

consistent changes in levels of N-cadherin were detected in lenses from 1-month-old heterozygous and homozygous fs380 mice (Fig. 9A), but N-cadherin levels were consistently decreased in 7.7-month-old homozygotes (Fig. 9B). The distributions of N-cadherin in epithelial and fiber cells were similar among all genotypes (Figs. 5, 7).

### Denucleation Is Unaffected by Expression of Cx46fs380

Since differentiation of lens cells (including degradation of nuclei) is affected by some connexin mutations,<sup>19,28,29</sup> we examined whether expression of fs380 affected denucleation of fiber cells by staining lens sections of all genotypes with 4',6-diamidino-2-phenylindole dihydrochloride (DAPI). In lens sections from wild-type mice, DAPI-stained nuclei localized in the epithelium and in the equatorial region, and nuclear remnants localized in differentiating fiber cells as expected. In fs380 heterozygotes and homozygotes, the distribution of nuclei and nuclear remnants was indistinguishable from that in wild-type lenses (Fig. 10).

### Expression of Cx46fs380 Leads to Changes in Some Crystallins

Formation of insoluble aggregates of crystallins is a common biochemical change in many kinds of cataracts.<sup>30</sup> To assess whether expression of fs380 affected the abundances, electrophoretic mobilities, and solubilities of crystallins, we analyzed water-soluble and -insoluble lens fractions by immunoblotting. At 1 month of age, immunoreactive  $\alpha$ A-,  $\alpha$ B-,  $\beta$ -, and  $\gamma$ -crystallins fractionated essentially completely within the soluble fractions (Fig. 11). The electrophoretic patterns of

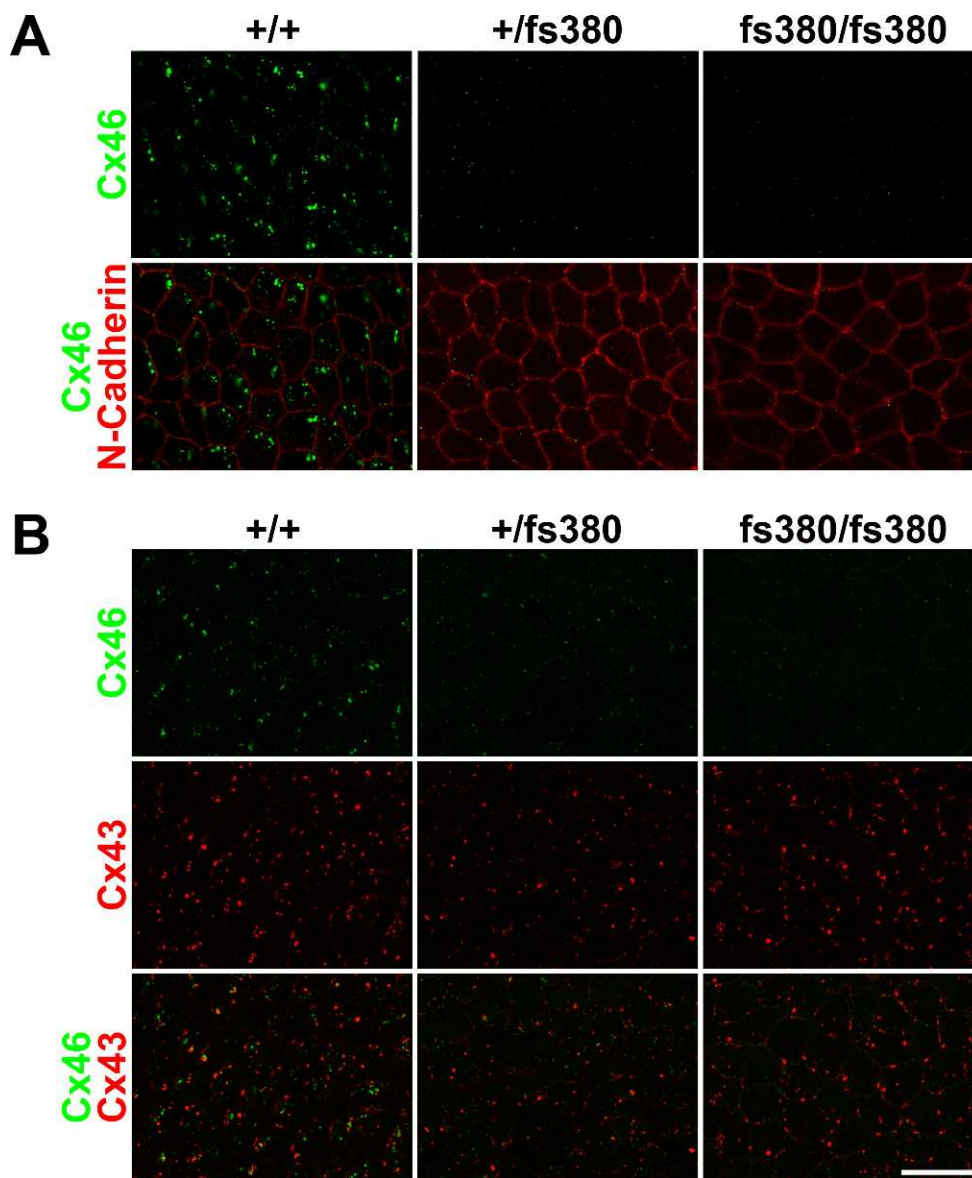


**FIGURE 5.** Immunoreactive Cx46 is decreased in epithelia from Cx46fs380-expressing lenses. Confocal images were obtained from whole mounts of lens epithelia from 1-month-old wild-type (+/+) and Cx46fs380 heterozygous (+/fs380) and homozygous (fs380/fs380) mice that were subjected to double-label immunofluorescence using anti-Cx46 and anti-N-cadherin antibodies (A) or anti-Cx43 and anti-Cx46 antibodies (B). Immunoreactivity for Cx46 is shown in green, and immunoreactivities for N-cadherin (A) and Cx43 (B) are shown in red. Scale bar: 23  $\mu$ m.

the crystallins did not differ between genotypes. At this age, the  $\alpha$ A-,  $\alpha$ B-, and  $\beta$ -crystallins were detected as single bands, while the  $\gamma$ -crystallins resolved as a triplet composed of a strong doublet and a faster-migrating faint band (Fig. 11).

In older mice (5.2 months), the total levels of  $\alpha$ A-,  $\alpha$ B-, and  $\gamma$ -crystallins did not differ among genotypes (Supplementary Fig. S3). The  $\alpha$ A- and  $\alpha$ B-crystallins were exclusively detected in the soluble fractions (Fig. 12A). Total levels of  $\beta$ -crystallins were consistently decreased in fs380-expressing lenses (Supplementary Fig. S3). While a proportion of the  $\beta$ -crystallins (2%) and  $\gamma$ -crystallins (21%) were detected in the insoluble fractions from the older wild-type lenses (Fig. 12), higher proportions of the  $\beta$ - and  $\gamma$ -crystallins were insoluble in fs380 lenses. The insolubility was more severe in homozygous than in heterozygous lenses (61% vs. 7% for  $\beta$ -crystallins, 76% vs. 32% for  $\gamma$ -crystallins) (Fig. 12).

In 5.2-month-old samples, the immunoblot pattern of  $\beta$ -crystallins (under reducing conditions) contained several bands with faster electrophoretic mobilities than intact monomeric  $\beta$ -crystallins (Fig. 12A) that likely correspond to truncated forms. The slowest of these faster-migrating forms (labeled “a” in Fig. 12A) fractionated with monomeric  $\beta$ -crystallins in the soluble fraction, but the fastest-migrating forms (labeled “b-d” in Fig. 12A) were insoluble (Fig. 12A). The total homogenate and the water-insoluble fraction of these older lenses also contained a  $\beta$ -crystallin band with a slower electrophoretic mobility (consistent with modification or cross-linking) that was barely detectable in wild-type and fs380 heterozygotes, but was more pronounced in fs380 homozygotes (arrow in Fig. 12A, Supplementary Fig. S3).

Immunoblots of  $\gamma$ -crystallins from the older lenses showed several bands in both the water-soluble and -insoluble fractions; however, the band with the highest electrophoretic

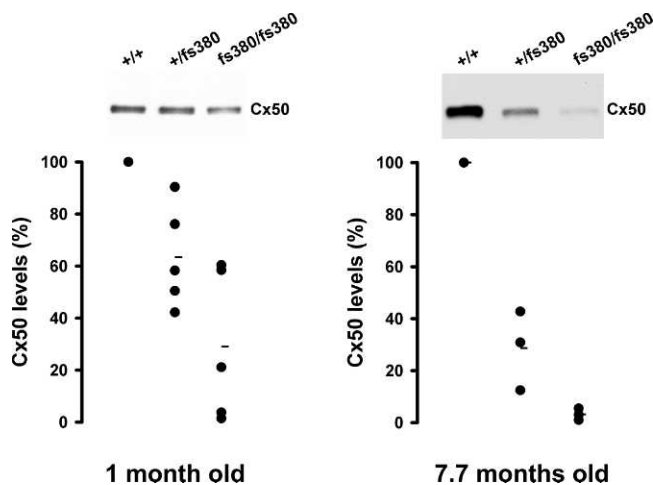


**FIGURE 6.** Levels of Cx50 decrease in Cx46fs380-expressing lenses. Immunoblots were performed on total lens homogenates of wild-type (+/+), heterozygous (+/fs380), and homozygous (fs380/fs380) mice at 1 or 7.7 months of age. The *graphs* show the quantification of the bands obtained in three to five independent experiments expressed as percentages of the values obtained from wild-type animals. The *short horizontal lines* indicate the average value for each genotype.

mobility was seen only in the water-insoluble fraction (Fig. 12A, asterisk). The difference in apparent molecular mass of the  $\gamma$ -crystallin bands is consistent with small truncations/modifications that alter electrophoretic mobility. We did not observe any immunoreactive fragments that were much smaller in apparent molecular mass.

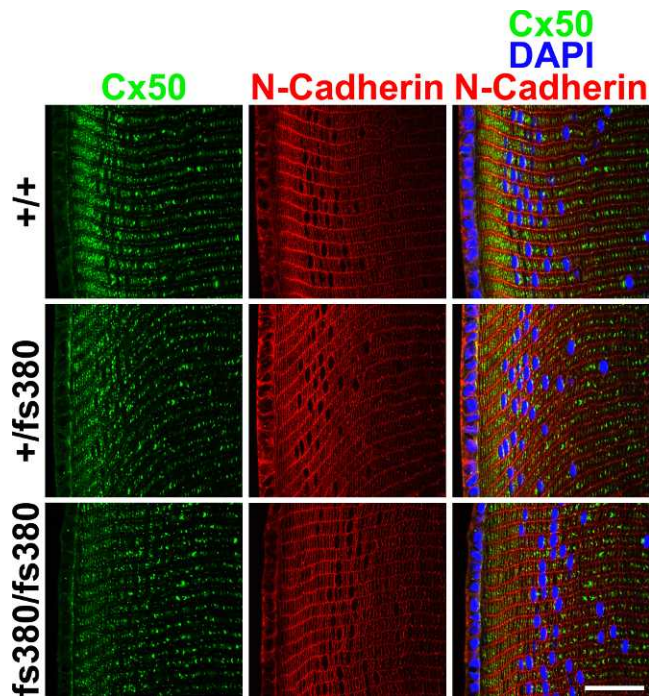


**FIGURE 7.** Expression of Cx46fs380 decreases the intensity of immunoreactive Cx50. Confocal images show the distributions of Cx50 (*green*) and N-cadherin (*red*) in sections of lenses from wild-type (+/+), heterozygous (+/fs380), and homozygous (fs380/fs380) mice at 1.1 months of age. Images on the *right* show the superposition of the Cx50 and N-cadherin immunoreactivities as well as DAPI staining of nuclei. *Scale bar*: 35  $\mu$ m.

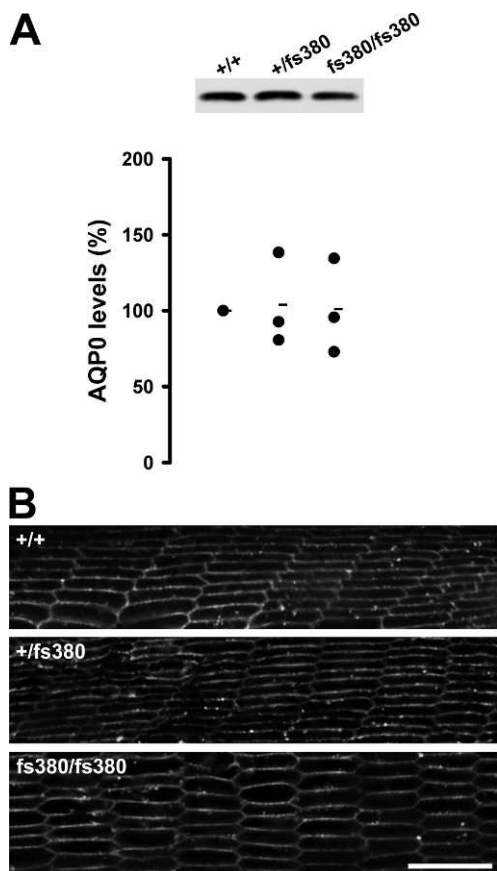


**FIGURE 8.** Levels and distribution of AQP0 are not affected in Cx46fs380-expressing lenses. (A) Immunoblots show levels of AQP0 in total lens homogenates from wild-type (+/+), heterozygous (+/fs380), and homozygous (fs380/fs380) mice at 7.7 months of age. The intensities of the immunoblot bands were quantified by densitometry in three independent experiments and graphed as percentages of the values obtained in wild-type animals. The *short horizontal lines* indicate the average value for each genotype. (B) Confocal images show the distribution of AQP0 immunoreactivity in cross sections from wild-type (+/+), heterozygous (+/fs380), and homozygous (fs380/fs380) lenses from 5.6-month-old mice. *Scale bar*: 14  $\mu$ m.

**DISCUSSION**

In this paper, we have shown that expression of the cataract-linked mutant Cx46fs380 induces progressive cataracts in heterozygous and homozygous mice. The lenses of these mice initially did not show opacities, but cataracts became apparent by 2 months in homozygotes and  $\geq 4$  months in heterozygotes. The first detection of cataracts is relatively later in these mice as compared with humans heterozygous for Cx46fs380, in whom cataracts are seen at birth or during infancy.<sup>11</sup> Beyond this difference, the cataract phenotype of fs380 mice resembles that described in affected members of the family carrying the Cx46 mutation. The lenses of these individuals contain coarse and granular opacities in the central zone (fetal nucleus) and fine dust-like opacities in peripheral regions (juvenile cortex).<sup>11</sup> In the fs380 mouse lenses, the opacities initially appeared punctate, but at later ages they became coarser and more extensive, suggesting the merging of distinct small opacities.

Notably, cellular and biochemical changes of some lens components were detectable long before the appearance of cataracts. One early change was the near absence of Cx46 in both heterozygotes and homozygotes. In cultured cells,

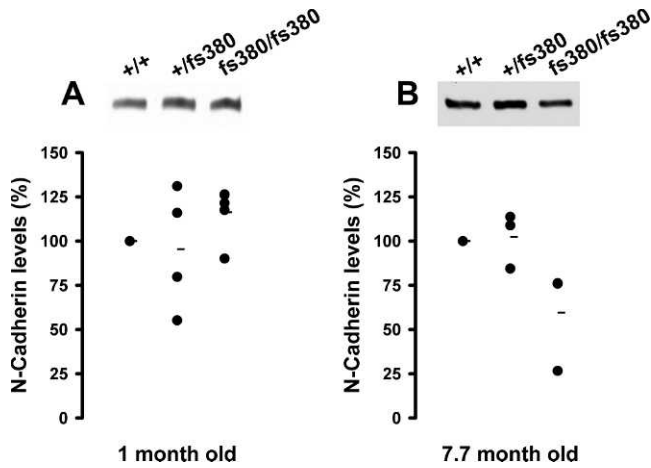


**FIGURE 9.** Levels of N-cadherin are decreased only in the lenses of older homozygous Cx46fs380 mice. Immunoblots show the levels of N-cadherin in total lens homogenates from wild-type (+/+), heterozygous (+/fs380), and homozygous (fs380/fs380) mice at 1 or 7.7 months of age. The *graphs* show the quantification of the bands obtained in at least three independent experiments expressed as percentages of the values obtained from wild-type animals. The *short horizontal lines* indicate the average value for each genotype.

Cx46fs380 does not traffic properly to the plasma membrane; rather it is confined within cytoplasmic compartments of the biosynthetic pathway.<sup>12</sup> In many cells, transmembrane and secreted proteins that do not traffic properly (like Cx46fs380) are recognized and degraded through “quality control” mechanisms. These mechanisms might produce significant Cx46fs380 degradation in lens cells (but their recognition/degradative capacity may have been overwhelmed in transfected HeLa cells). Moreover, in the lens, organelles (including the endoplasmic reticulum, Golgi, and other components of the secretory pathway) are degraded as fiber cells mature. Thus, quality control mechanisms and organelle degradation could explain the near absence of Cx46 in fs380 homozygous lenses that produce only the mutant protein. Other expression studies also suggest increased degradation of this mutant, since levels of <sup>35</sup>S-methionine-labeled Cx46fs380 are much lower than those of wild-type Cx46 in oocytes injected with equal amounts of wild-type or Cx46fs380 complementary RNAs.<sup>31</sup> In

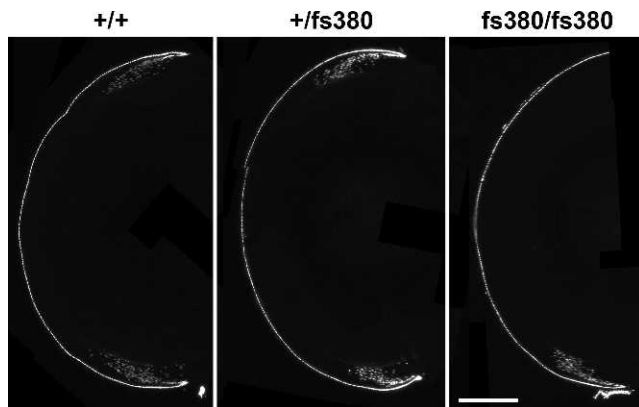


**FIGURE 10.** The distribution of nuclei and nuclear fragments is similar in wild-type and Cx46fs380-expressing lenses. Photomicrographs show the distribution of DAPI-stained nuclei (and fragments) in longitudinal sections of lenses from 1-month-old wild-type (+/+), heterozygous (+/fs380) and homozygous (fs380/fs380) mice. *Scale bar:* 530  $\mu$ m.

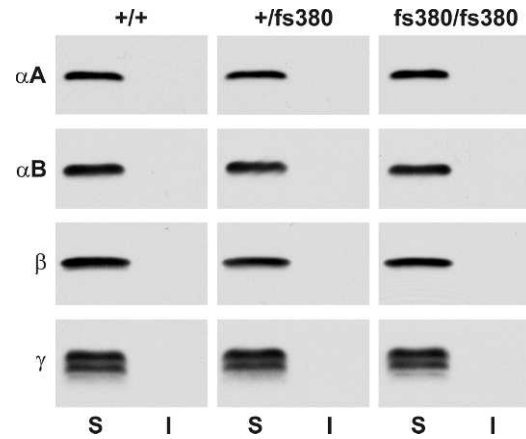


**FIGURE 11.** Expression of Cx46fs380 does not affect crystallin solubility at 1 month of age. Water-soluble (S) and -insoluble (I) fractions were prepared from total lens homogenates of 1-month-old wild-type (+/+), heterozygous (+/fs380), and homozygous (fs380/fs380) mice. Immunoblots were performed using anti- $\alpha$ A-, anti- $\alpha$ B-, anti- $\beta$ -, or anti- $\gamma$ -crystallin antibodies.

heterozygotes, the large decrease in Cx46 levels is likely caused by extensive oligomerization between wild-type and mutant Cx46, resulting in oligomers with impaired trafficking that are degraded. This hypothesis is supported by the immunofluorescence results showing very few Cx46-immunoreactive puncta at the plasma membrane of lens cells from fs380 mice. Thus, a major cause of the cataracts in heterozygous and homozygous fs380 mice is the absence of Cx46 protein in all lens cells.

Our results in the Cx46fs380 knockin mouse model contrast with some observations made in Cx46KO mice. Only homozygous Cx46KO animals (not heterozygotes) develop cataracts that are detectable by 2 to 3 weeks of age.<sup>9</sup> In contrast, we detected opacities in both heterozygous and homozygous fs380 mice, and at later ages. The cataracts were localized in an anterior region of the nucleus in the fs380 mice, whereas they are nuclear in Cx46KO mice. One-month-old fs380 mice did not have cataracts even though Cx46 levels were nearly undetectable (as in homozygous Cx46-null animals), possibly reflecting the contributions of other genes to lens transparency. The Cx46KO and fs380 mice were generated in embryonic stem cells of the 129/SvJ mouse strain, which carries a mutation in the phakinin (CP49) gene.<sup>32</sup> Unlike the Cx46KO mice, we bred this mutation out from our fs380 mouse colony. Indeed, the severity of the cataract in Cx46-null mice is far milder in a C57BL/6J background,<sup>33</sup> a mouse strain that does not carry the CP49 mutation.<sup>32</sup>

Expression of Cx46fs380 caused a decrease in Cx50 levels and in the intensity and density of the immunofluorescent puncta. Because Cx46 and Cx50 can form mixed hexamers (or heteromeric connexons),<sup>26</sup> it is likely that the decreased Cx50 in Cx46fs380 mice resulted from degradation of oligomers containing both wild-type Cx50 and Cx46fs380. In contrast, Cx50 levels were not reduced in the lens cortex of Cx46KO mice, but these samples contained a faster-migrating form of Cx50<sup>34</sup> that we did not detect in fs380 animals. It is noteworthy that another connexin mutant associated with autosomal dominant cataracts (Cx50D47A) also affected the coexpressed lens fiber connexin (in this case, Cx46),<sup>19</sup> suggesting that this may be a common mechanism by which autosomal dominant connexin mutants lead to disease.

The reductions of both Cx46 and Cx50 in fs380 lenses suggest a comparison with double Cx46-Cx50 knockout mice. In young double-null animals, cataracts were initially observed

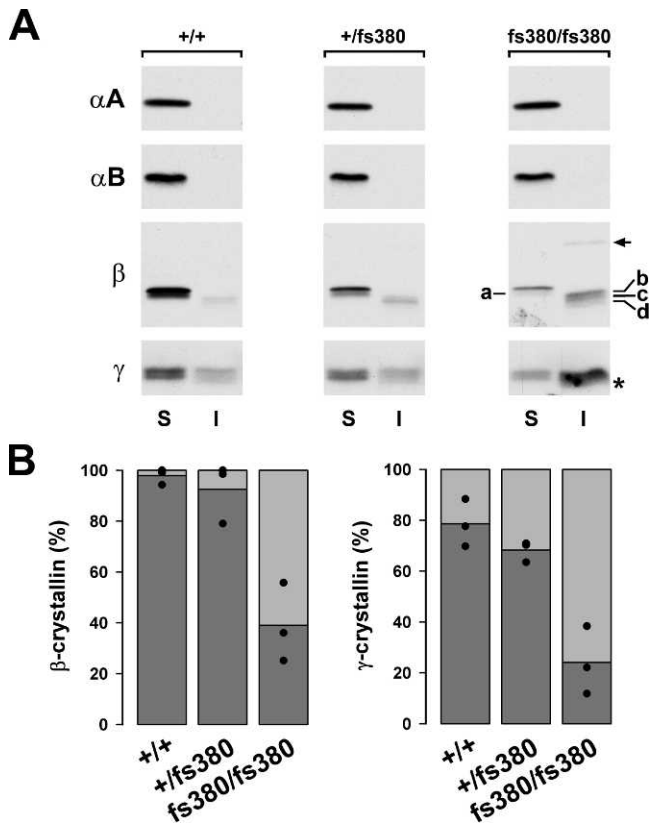


**FIGURE 12.** In lenses of older mice, expression of Cx46fs380 increases the insolubility of β- and γ-crystallins. **(A)** Water-soluble (S) and -insoluble (I) fractions were prepared from total lens homogenates of 5.2-month-old wild-type (+/+), heterozygous (+/fs380), and homozygous (fs380/fs380) mice, followed by immunoblotting using anti-αA-, anti-αB-, anti-β-, or anti-γ-crystallin antibodies. Immunoreactive β-crystallin bands of faster electrophoretic mobilities compared to the full-length protein are labeled “a” through “d” for the fs380 homozygote blot; the “a” band is water soluble, whereas the “b” through “d” bands are water insoluble. A β-crystallin band with slower electrophoretic mobility (detected mainly in the homozygote sample) is indicated by the *arrow*. The immunoreactive γ-crystallin band with the fastest electrophoretic mobility (indicated by the *asterisk*) is water insoluble. **(B)** Bar graphs represent the average of the relative proportions of β- and γ-crystallin in the soluble (*dark gray*) and insoluble (*light gray*) fractions after quantification of the bands detected in three independent experiments (*black circles*).

as Yshaped at the anterior suture,<sup>35</sup> similar to the cataracts in heterozygous fs380 animals. However, at comparable ages, the cataracts in fs380 mice were much milder than the dense nuclear cataract observed in the double knockout animals. Cataracts were first observed at postnatal days 2 to 7 in the double-null mice<sup>35</sup> as compared to much later in fs380 mice (2 months in homozygotes and ≥4 months in heterozygotes). The milder cataract in fs380 mice probably reflects the presence of functional Cx50 as compared to its complete absence in double knockout mice. Additionally, genetic differences contribute to the increased severity of the cataract.

Cx46fs380 expression also affected another membrane protein. Levels of N-cadherin were decreased in old homozygotes. Since N-cadherin is an adhesion molecule present in all lens cells,<sup>27</sup> its decrease may reflect a deterioration of adherens junctions in these mutant lenses. However, the general distribution of N-cadherin was not altered.

Expression of Cx46fs380 did not have obvious effects on the growth or differentiation of lens cells. The sizes of the

lenses and the process of denucleation appeared normal in mice carrying the Cx46fs380 mutant allele. These results are similar to those reported for Cx46KO mice,<sup>9,36</sup> but they contrast with the smaller lenses and varying degrees of impaired denucleation observed in Cx50-null mice and some mutant Cx50 animals.<sup>10,18,19,28,29,37,38</sup> These findings are consistent with the hypothesis that Cx46 and Cx50 are important for maintaining lens transparency, while Cx50 also contributes to lens cell proliferation and differentiation.<sup>19,39</sup>

With the development of cataracts, the fs380 mice exhibited alterations of crystallins. High molecular weight insoluble aggregates containing crystallins or crystallin-derived peptides are commonly found in cataracts regardless of etiology.<sup>30,40</sup> In the fs380 mice, the water solubility of αA-, αB-, β-, or γ-crystallins was unaffected at 1 month of age. In contrast, the water insolubility of β- and γ-crystallins (but not αA or αB) was increased in older (5.2 months) heterozygous and homozygous fs380 lenses. It is not surprising that the homozygous fs380 mice (which had a more severe cataract) had more insoluble β- and γ-crystallins than heterozygotes, since the abundance of insoluble crystallins frequently correlates with cataract severity. Gong et al.<sup>9</sup> also found a decrease in water-soluble β- and γ-crystallins in the lenses of 4-month-old homozygous Cx46KO mice, but (unlike the fs380 lenses) it was accompanied by the presence of water-insoluble α-crystallins. It is interesting that α-crystallins remained water soluble in fs380 lenses, since these proteins with chaperone functions contribute to insoluble aggregates in many kinds of cataractous lenses.<sup>41–43</sup>

Crystallins undergo several modifications that are more prevalent with cataract formation.<sup>40,44</sup> Some modifications affect crystallin stability, ultimately leading to their precipitation/aggregation.<sup>40,45</sup> We observed decreased total levels of β-crystallins in older fs380 mice and an increase in slower- and faster-migrating electrophoretic forms. These observations are consistent with degradation, modification (or protein cross-linking), and cleavage/truncation of the proteins. Interestingly, the slowest- and fastest-migrating forms were water insoluble, whereas intact, monomeric β-crystallins were water soluble. Although the exact roles of β-crystallins and their modified forms in the lens are undefined,<sup>45</sup> these changes deserve future investigation as potential contributors to cataractogenesis, especially since several cataracts have been linked to β-crystallin missense mutations.<sup>5</sup> We also detected several γ-crystallin bands that likely correspond to modified forms. However, we did not find the small (11-kDa) fragment generated by calpain-dependent cleavage related to increased lens calcium levels in homozygous Cx46KO mice from the mixed 129SvJae X C57BL/6J background,<sup>9,46,47</sup> suggesting that this process is not occurring in the fs380 lenses.

Reduced connexin function is probably a substantial mechanistic component of the pathology in the fs380 lenses. Studies of adult lenses have suggested that Cx43 is the main connexin providing intercellular communication in lens epithelial cells (reviewed in Ref. 48). Investigations of Cx50- and Cx46-null mice implicate Cx46 and Cx50 as critical for intercellular communication in differentiating fiber cells, with Cx46 being the major contributor in mature fiber cells.<sup>8</sup> These studies imply that the decreased levels of Cx46 in fs380 lenses would lead to a major decrease in intercellular communication between mature fiber cells. The delayed appearance of the cataract in heterozygous mice implies a contribution of Cx50 to intercellular coupling in mature fibers. As the mice aged and Cx50 levels also decreased, intercellular communication would become more compromised and reduced in differentiating fiber cells as well. Decreased connexin-mediated intercellular communication could account for the development and progression of cataracts in fs380 mice. However, it does not



explain the delayed appearance of the cataract. There must be compensatory responses that differ between the fs380 and the Cx46-null lenses. Although expression of a mutant protein may have toxic cellular effects, it may also induce adaptive changes that allow adequate cell homeostasis (despite reduced intercellular communication) to maintain lens transparency temporarily. The adaptive responses would also have to compensate for altered transmembrane currents in fs380 lens cells, since Cx46 also forms “hemichannels.”<sup>25,49</sup> Such adaptive responses may not be triggered in the Cx46KO mice, which lack expression of the wild-type protein.

In summary, our studies on the knockin Cx46fs380 mice demonstrate that heterozygous (and homozygous) fs380 mice develop cataracts consistent with the autosomal inheritance of this trait in humans. The lenses of fs380 mice exhibit biochemical abnormalities before the presence of detectable opacities. Thus, these mice will be a useful model to study the progression of changes in the lens during cataractogenesis resulting from expression of an abnormal major lens membrane protein.

### Acknowledgments

The authors thank Alexandra Lichtenstein and Rebecca Hernandez for their participation in the early phases of this project.

Supported by a Children’s Research Foundation Grant (VMB) and National Institutes of Health Grants RO1EY08368 (ECB) and UL1TR000430 (core subsidy, VMB).

Disclosure: **V.M. Berthoud**, None; **P.J. Minogue**, None; **H. Yu**, None; **J.I. Snabb**, None; **E.C. Beyer**, None

### References

- Resnikoff S, Pascolini D, Etya’ale D, et al. Global data on visual impairment in the year 2002. *Bull World Health Organ.* 2004; 82:844–851.
- Pascolini D, Mariotti SP. Global estimates of visual impairment: 2010. *Br J Ophthalmol.* 2012;96:14–18.
- Bourne RR, Jonas JB, Flaxman SR, et al.; Vision Loss Expert Group of the Global Burden of Disease Study. Prevalence and causes of vision loss in high-income countries and in Eastern and Central Europe: 1990–2010. *Br J Ophthalmol.* 2014;98: 629–638.
- Shiels A, Bennett TM, Hejtmancik JK. *Cat-Map*: putting cataract on the map. *Mol Vis.* 2010;16:2007–2015.
- Churchill A, Graw J. Clinical and experimental advances in congenital and paediatric cataracts. *Philos Trans R Soc Lond B Biol Sci.* 2011;366:1234–1249.
- Beyer EC, Ebihara L, Berthoud VM. Connexin mutants and cataracts. *Front Pharmacol.* 2013;4:43.
- Goodenough DA. The crystalline lens. A system networked by gap junctional intercellular communication. *Semin Cell Biol.* 1992;3:49–58.
- Mathias RT, White TW, Gong X. Lens gap junctions in growth, differentiation, and homeostasis. *Physiol Rev.* 2010;90:179–206.
- Gong X, Li E, Klier G, et al. Disruption of  $\alpha_3$  connexin gene leads to proteolysis and cataractogenesis in mice. *Cell.* 1997; 91:833–843.
- White TW, Goodenough DA, Paul DL. Targeted ablation of connexin50 in mice results in microphthalmia and zonular pulverulent cataracts. *J Cell Biol.* 1998;143:815–825.
- Mackay D, Ionides A, Kibar Z, et al. Connexin46 mutations in autosomal dominant congenital cataract. *Am J Hum Genet.* 1999;64:1357–1364.
- Minogue PJ, Liu X, Ebihara L, Beyer EC, Berthoud VM. An aberrant sequence in a connexin46 mutant underlies congenital cataracts. *J Biol Chem.* 2005;280:40788–40795.
- Kalcheva N, Qu J, Sandeep N, et al. Gap junction remodeling and cardiac arrhythmogenesis in a murine model of oculodentodigital dysplasia. *Proc Natl Acad Sci U S A.* 2007;104: 20512–20516.
- Dobrowolski R, Sasse P, Schrickel JW, et al. The conditional connexin43G138R mouse mutant represents a new model of hereditary oculodentodigital dysplasia in humans. *Hum Mol Genet.* 2008;17:539–554.
- Schütz M, Auth T, Gehrt A, et al. The connexin26 S17F mouse mutant represents a model for the human hereditary keratitis-ichthyosis-deafness syndrome. *Hum Mol Genet.* 2011;20:28–39.
- Schütz M, Scimemi P, Majumder P, et al. The human deafness-associated connexin 30 T5M mutation causes mild hearing loss and reduces biochemical coupling among cochlear non-sensory cells in knock-in mice. *Hum Mol Genet.* 2010;19: 4759–4773.
- Mese G, Sellitto C, Li L, et al. The Cx26-G45E mutation displays increased hemichannel activity in a mouse model of the lethal form of keratitis-ichthyosis-deafness syndrome. *Mol Biol Cell.* 2011;22:4776–4786.
- Xia CH, Chang B, DeRosa AM, Cheng C, White TW, Gong X. Cataracts and microphthalmia caused by a Gja8 mutation in extracellular loop 2. *PLoS One.* 2012;7:e52894.
- Berthoud VM, Minogue PJ, Yu H, Schroeder R, Snabb JI, Beyer EC. Connexin50D47A decreases levels of fiber cell connexins and impairs lens fiber cell differentiation. *Invest Ophthalmol Vis Sci.* 2013;54:7614–7622.
- Chung J, Berthoud VM, Novak L, et al. Transgenic overexpression of connexin50 induces cataracts. *Exp Eye Res.* 2007;84: 513–528.
- Minogue PJ, Tong JJ, Arora A, et al. A mutant connexin50 with enhanced hemichannel function leads to cell death. *Invest Ophthalmol Vis Sci.* 2009;50:5837–5845.
- Berthoud VM, Singh R, Minogue PJ, Ragsdale CW, Beyer EC. Highly restricted pattern of connexin36 expression in chick somite development. *Anat Embryol (Berl).* 2004;209:11–18.
- Beyer EC, Kistler J, Paul DL, Goodenough DA. Antisera directed against connexin43 peptides react with a 43-kD protein localized to gap junctions in myocardium and other tissues. *J Cell Biol.* 1989;108:595–605.
- Koval M, Harley JE, Hick E, Steinberg TH. Connexin46 is retained as monomers in a *trans*-Golgi compartment of osteoblastic cells. *J Cell Biol.* 1997;137:847–857.
- Paul DL, Ebihara L, Takemoto LJ, Swenson KI, Goodenough DA. Connexin46, a novel lens gap junction protein, induces voltage-gated currents in nonjunctional plasma membrane of *Xenopus* oocytes. *J Cell Biol.* 1991;115:1077–1089.
- Jiang JX, Goodenough DA. Heteromeric connexons in lens gap junction channels. *Proc Natl Acad Sci U S A.* 1996;93:1287–1291.
- Beebe DC, Vasiliev O, Guo J, Shui YB, Bassnett S. Changes in adhesion complexes define stages in the differentiation of lens fiber cells. *Invest Ophthalmol Vis Sci.* 2001;42:727–734.
- Graw J, Löster J, Soewarto D, et al. Characterization of a mutation in the lens-specific MP70 encoding gene of the mouse leading to a dominant cataract. *Exp Eye Res.* 2001;73: 867–876.
- Alapure BV, Stull JK, Firtina Z, Duncan MK. The unfolded protein response is activated in connexin 50 mutant mouse lenses. *Exp Eye Res.* 2012;102:28–37.
- Moreau KL, King JA. Protein misfolding and aggregation on cataract disease and prospects for prevention. *Trends Mol Med.* 2012;18:273–282.
- Pal JD, Liu X, Mackay D, et al. Connexin46 mutations linked to congenital cataract show loss of gap junction channel function. *Am J Physiol Cell Physiol.* 2000;279:C596–C602.

32. Alizadeh A, Clark J, Seeberger T, Hess J, Blankenship T, FitzGerald PG. Characterization of a mutation in the lens-specific CP49 in the 129 strain of mouse. *Invest Ophthalmol Vis Sci.* 2004;45:884-891.
33. Gong X, Agopian K, Kumar NM, Gilula NB. Genetic factors influence cataract formation in  $\alpha_3$  connexin knockout mice. *Dev Gen.* 1999;24:27-32.
34. Gong X, Baldo GJ, Kumar NM, Gilula NB, Mathias RT. Gap junctional coupling in lenses lacking  $\alpha_3$  connexin. *Proc Natl Acad Sci U S A.* 1998;95:15303-15308.
35. Xia CH, Cheng C, Huang Q, et al. Absence of  $\alpha_3$  (Cx46) and  $\alpha_8$  (Cx50) connexins leads to cataracts by affecting lens inner fiber cells. *Exp Eye Res.* 2006;83:688-696.
36. Dunia I, Cibert C, Gong X, et al. Structural and immunocytochemical alterations in eye lens fiber cells from Cx46 and Cx50 knockout mice. *Eur J Cell Biol.* 2006;85:729-752.
37. Rong P, Wang X, Niesman I, et al. Disruption of *Gja8* ( $\alpha_8$  connexin) in mice leads to microphthalmia associated with retardation of lens growth and lens fiber maturation. *Development.* 2002;129:167-174.
38. Xia CH, Liu H, Cheung D, et al. Diverse gap junctions modulate distinct mechanisms for fiber cell formation during lens development and cataractogenesis. *Development.* 2006;133:2033-2040.
39. Sellito C, Li L, White TW. Connexin50 is essential for normal postnatal lens cell proliferation. *Invest Ophthalmol Vis Sci.* 2004;45:3196-3202.
40. Sharma KK, Santhoshkumar P. Lens aging: Effects of crystallins. *Biochim Biophys Acta.* 2009;1790:1095-1108.
41. Kamei A, Iwata S, Horwitz J. Characterization of water-insoluble proteins in human lens nuclei. *Jpn J Ophthalmol.* 1987;31:433-439.
42. Horwitz J.  $\alpha$ -Crystallin can function as a molecular chaperone. *Proc Natl Acad Sci U S A.* 1992;89:10449-10453.
43. Harrington V, Srivastava OP, Kirk M. Proteomic analysis of water insoluble proteins from normal and cataractous human lenses. *Mol Vis.* 2007;13:1680-1694.
44. Truscott JW, Friedrich MG. Old proteins and the Achilles heel of mass spectrometry. The role of proteomics in the etiology of human cataract. *Proteomics Clin Appl.* 2014;1:1-9.
45. Lampi KJ, Wilmarth PA, Murray MR, David LL. Lens  $\beta$ -crystallins: The role of deamidation and related modifications in aging and cataract. *Prog Biophys Mol Biol.* 2014;115:21-31.
46. Baruch A, Greenbaum D, Levy ET, et al. Defining a link between gap junction communication, proteolysis, and cataract formation. *J Biol Chem.* 2001;276:28999-29006.
47. Tang Y, Liu X, Zoltoski RK, et al. Age-related cataracts in  $\alpha_3$ Cx46-knockout mice are dependent on a calpain 3 isoform. *Invest Ophthalmol Vis Sci.* 2007;48:2685-2694.
48. Berthoud VM, Minogue PJ, Osmolak P, Snabb JI, Beyer EC. Roles and regulation of lens epithelial cell connexins. *FEBS Lett.* 2014;588:1297-1303.
49. Ebihara L, Tong JJ, Vertel B, White TW, Chen TL. Properties of connexin 46 hemichannels in dissociated lens fiber cells. *Invest Ophthalmol Vis Sci.* 2011;52:882-889.